

Muon-spin relaxation measurements on the dimerized spin-1/2 chains $\text{NaTiSi}_2\text{O}_6$ and TiOCl

P. J. Baker,¹ S. J. Blundell,¹ F. L. Pratt,² T. Lancaster,¹ M. L. Brooks,¹ W. Hayes,¹ M. Isobe,³ Y. Ueda,³ M. Hoinkis,^{4,5} M. Sing,⁴ M. Klemm,⁵ S. Horn,⁵ and R. Claessen⁴

¹Clarendon Laboratory, University of Oxford, Parks Road, Oxford OX1 3PU, United Kingdom

²ISIS Muon Facility, ISIS, Chilton, Oxon., OX11 0QX, United Kingdom

³Institute for Solid State Physics, University of Tokyo,

5-1-5 Kashiwanoha, Kashiwa, Chiba 277-8581. Japan

⁴Experimentelle Physik 4, Universität Würzburg, D-97074 Würzburg, Germany

⁵Experimentalphysik II, Universität Augsburg, D-86159 Augsburg, Germany

(Dated: February 6, 2008)

We report muon spin relaxation (μ SR) and magnetic susceptibility investigations of two Ti^{3+} chain compounds which each exhibit a spin gap at low temperature, $\text{NaTiSi}_2\text{O}_6$ and TiOCl . From these we conclude that the spin gap in $\text{NaTiSi}_2\text{O}_6$ is temperature independent, with a value of $2\Delta = 660(50)$ K, arising from orbital ordering at $T_{\text{OO}} = 210$ K; the associated structural fluctuations activate the muon spin relaxation rate up to temperatures above 270 K. In TiOCl we find thermally activated spin fluctuations corresponding to a spin gap $2\Delta = 420(40)$ K below $T_{c1} = 67$ K. We also compare the methods used to extract the spin gap and the concentration of free spins within the samples from μ SR and magnetic susceptibility data.

PACS numbers: 76.75.+i, 75.50.Ee, 75.10.Jm, 75.40.Cx

The interplay between spin, charge, and orbital degrees of freedom is particularly subtle in strongly-correlated oxides containing octahedrally-coordinated Ti^{3+} ions (t_{2g}^1). Such compounds are typically insulators because the $S = 1/2$ spins are localized in the t_{2g}^1 orbitals. In oxides containing chains of Ti^{3+} ions, superexchange via oxygen gives rise to antiferromagnetic coupling. A well known instability that can affect half-integer spin chains is the spin-Peierls (SP) transition¹, in which magnetoelectric coupling dimerizes the chain and allows a spin-gap, 2Δ , to open below a characteristic temperature, T_{SP} , resulting in a spin-singlet ground state. (e.g. $T_{\text{SP}} = 14$ K for CuGeO_3 ², $T_{\text{SP}} = 18$ K for $\text{MEM}(\text{TCNQ})_2$ ³) In contrast, for integer spins a Haldane gap will be present, precluding any low temperature instability⁴.

Recently, two oxides, $\text{NaTiSi}_2\text{O}_6$ (NTSO) and TiOCl , have been intensively studied because they undergo dimerization transitions at unusually high temperatures. NTSO has the pyroxene structure with chains of TiO_6 octahedra that are only weakly coupled to one another⁵. TiOCl has TiO bilayers within the ab plane, well separated by Cl^- ions. At low temperature dimerized chains of Ti^{3+} ions form along the b axis, with their spins coupled by direct exchange⁶. The magnetic susceptibility, χ , drops sharply at 210 K for NTSO⁵ and 67 K for TiOCl ⁷ due to the opening of a spin gap. However, for both compounds, the ratio of the spin gap (which we will quote in Kelvin) to the dimerization temperature is larger than for the canonical SP case (for which $2\Delta/T_{\text{SP}} = 3.53$)¹, demonstrating that the dimerization transitions are more complex than the canonical SP case, and pointing to the possible rôle of orbital physics.

X-ray diffraction studies of NTSO show that the Ti^{3+} chains dimerize below 210 K.⁸ Phonon anomalies measured using Raman scattering⁹ are consistent with the

dimerization being driven by an orbital ordering at $T_{\text{OO}} = 210$ K, below which the system is condensed in one of two possible orbitally ordered spin-singlet states, breaking translational symmetry. This model is supported by a number of theoretical studies^{10,11,12}, although a composite $S = 1$ Haldane chain ground state, with spin-triplet dimers of ferromagnetically coupled Ti^{3+} spins, has also been proposed¹³. (See also Refs. 11, 14.)

Unusually, the dimerization of TiOCl occurs in two stages. There is a second order phase transition at $T_{c2} = 91$ K into an incommensurate dimerized phase, and a first order transition at $T_{c1} = 67$ K into a commensurate SP phase^{6,7,15,16,17}. Although early work suggested that orbital fluctuations may play a dominant rôle in driving the transition^{16,18,19,20}, recent experiments have ruled this out^{17,21,22}. In particular, optical measurements, in combination with a cluster calculation, revealed that the crystal field splitting is large enough to quench the orbital degree of freedom¹⁷. It appears that frustration between the two staggered chains in the bilayer crystal structure of TiOCl leads to an incommensurate SP state between T_{c1} and T_{c2} ^{15,23,24}. The magnitude of the spin gap has previously been measured using optical techniques^{18,25} and NMR¹⁵. The former suggest a value of $2\Delta \sim 430$ K, whereas the latter gave a value of $\Delta = 430 \pm 60$ K, which is very large compared to the observed transition temperatures.

Muon spin relaxation (μ SR) experiments²⁶ probe magnetic ordering and dynamics from a microscopic viewpoint. The applicability of this technique to spin-gapped systems has been demonstrated by studies of the canonical SP compounds CuGeO_3 ^{27,28}, and $\text{MEM}(\text{TCNQ})_2$ ^{29,30}, and the Haldane chain compound Y_2BaNiO_5 ³¹. In this paper we present the results of μ SR

experiments on NTSO and TiOCl. We also made magnetic susceptibility measurements using a SQUID magnetometer that allow us to compare our results with previous data^{5,7,17}. We have measured the magnitude of the spin gap and found the concentration of unpaired spins in the dimerized state.

Our polycrystalline sample of NTSO was prepared by a solid-state reaction⁵ of $\text{Na}_2\text{TiSi}_4\text{O}_{11}$, Ti, and TiO_2 . The sample of TiOCl was composed of small single crystals synthesized using standard vapour-transport techniques³² from TiO_2 and TiCl_3 . Our μSR experiments were carried out using the MuSR and ARGUS spectrometers at the ISIS facility, United Kingdom. These were done in zero applied magnetic field (ZF) and in small magnetic fields along the axis of the initial muon spin polarization. Spin-polarized positive muons (μ^+ , mean lifetime $2.2\ \mu\text{s}$, momentum $28\ \text{MeV}/c$, $\gamma_\mu = 2\pi \times 135.5\ \text{MHz T}^{-1}$) were implanted into the polycrystalline samples where they stop within $\sim 1\ \text{ns}$. The decay positron asymmetry function²⁶, $A(t)$, is proportional to the average spin polarization of the muons stopped within the sample. Examples of the measured asymmetry spectra are presented in Fig. 1.

The absence of coherent muon precession, which would be indicative of a spontaneous magnetic field, together with the observation that both high and low temperature spectra relax to the same value with negligible missing asymmetry (Fig. 1), excludes the presence of long-range magnetic order in either material. The form of the muon spin relaxation is dependent on the distribution and time-dependence of the local magnetic fields around the site where the muon is implanted. In spin-gapped materials we write $A(t)$ as a product of relaxation functions^{27,29,30}. We approximate a Gaussian Kubo-Toyabe function²⁶ (which models the Gaussian distribution of randomly orientated nuclear spins) using $\exp[-(\sigma t)^2]$, use $\exp(-\lambda t)$ to describe the depolarization due to fluctuating electronic spins, and add a constant background A_{BG} to describe those muons landing outside the sample; giving a fitting function:

$$A(t) = A(0) \exp[-(\sigma t)^2] \exp(-\lambda t) + A_{\text{BG}}. \quad (1)$$

At high temperature the relaxation due to the fluctuations of nuclear spins dominates. Because the observed value of σ is small we do not see a recovery in the muon asymmetry at longer times; this is also due, in part, to the presence of the electronic fluctuations. Fitting the data with σ as a free parameter over the whole temperature range, $15 - 340\ \text{K}$, showed that in NTSO it was, within experimental error, temperature independent and it was subsequently fixed at $\sigma = 0.06\ \text{MHz}$. In TiOCl the situation is more complicated³³. The values of σ obtained for TiOCl are shown in the inset to Fig. 3(a).

The relaxation of the muon spin due to the fluctuating electronic spins changes significantly as a function of temperature, dominating the relaxation at low temperature. Providing the electronic spin-fluctuation rate ν is fast compared with $\sqrt{\langle B_\mu^2 \rangle}/\gamma_\mu$, where B_μ is the fluctu-

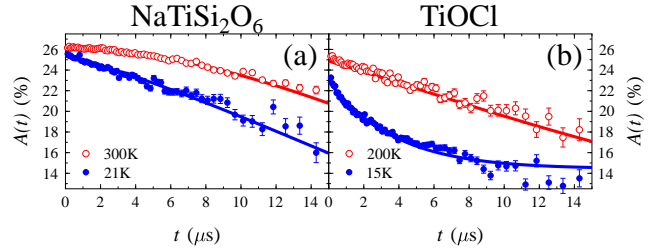


FIG. 1: (Color online) Examples of muon decay asymmetry data in (a) $\text{NaTiSi}_2\text{O}_6$ and (b) TiOCl, with fits to Eq. 1.

ating field at the muon-site due to the electronic spins (the fast-fluctuation regime), then³⁰ $\lambda \propto 1/\nu$. The temperature variation of λ is shown in Fig. 2(a) (NTSO) and Fig. 3(a) (TiOCl). At low temperature, one possible relaxation mechanism for the muon spin is via thermally activated electronic spins fluctuating across the spin gap³⁴. This would lead to the relaxation rate $\lambda(T)$:

$$\lambda(T) = A \exp(2\Delta/T), \quad (2)$$

where A is a constant. X-ray measurements show that the degree of dimerization is essentially constant below T_{OO} (NTSO)⁸ and T_{c1} (TiOCl)²³, so we take Δ as a constant for each compound. If an additional temperature-independent relaxation mechanism is present then:

$$\lambda(T) = \lambda_0/[1 + B \exp(-2\Delta/T)], \quad (3)$$

where B is a constant.

For NTSO, Eq. 3 fits the data quite well at temperatures up to T_{OO} and even slightly above, suggesting that the relevant spin fluctuations in the paramagnetic state are controlled by a similar energy scale (in fact, the antiferromagnetic exchange $J \sim \Delta$)¹¹. There is no sharp change in λ at T_{OO} , as might be expected if Haldane chains¹³ formed at that temperature, since the local field at the muon site should change significantly in that case. The best fit to the data, found by including points up to 270 K, gives $2\Delta = 660 \pm 60\ \text{K}$.

In contrast, for TiOCl, the behavior is more complex. We see no significant changes in λ either at T_{c2} or at $T^* \simeq 120\ \text{K}$, the temperature at which a pseudogap has been proposed^{15,18,25}. However, λ rises sharply below T_{c1} and we are able to fit the λ values between 58 K and 68.2 K to Eq. 2 yielding $2\Delta = 420 \pm 40\ \text{K}$. This value is in agreement with the magnitude of the spin gap previously measured using other techniques^{15,18,25,35}. At lower temperatures, λ shows a much slower increase with decreasing temperature, and Eq. 1 only poorly describes the data. Instead, a square root exponential, $\exp(-\sqrt{\lambda}t)$, as would be expected for a dilute distribution of slowly fluctuating electronic moments³⁶, provides a better description of the data. This interpretation is supported by longitudinal-field measurements which imply that the fluctuations leave the fast fluctuation regime when $\lambda \gtrsim 0.16\ \text{MHz}$ (In contrast, similar measurements

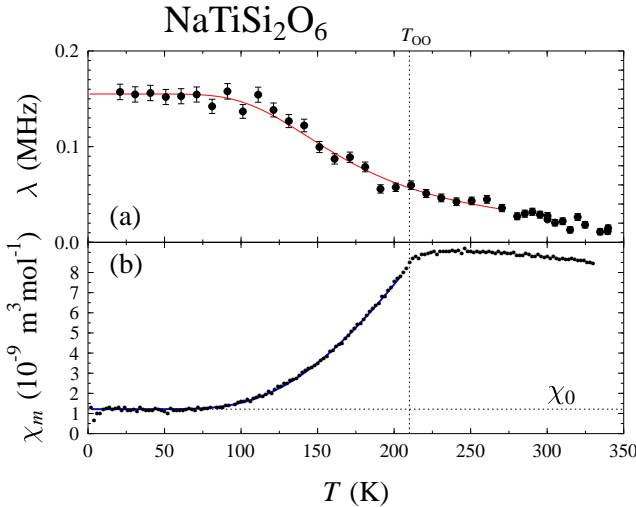


FIG. 2: (Color online) Fitted data for $\text{NaTiSi}_2\text{O}_6$. (a) Electronic relaxation rate, λ (Eq. 1). The red solid line is a fit to Eq. 3. (b) Magnetic susceptibility, χ_m , after subtraction of the low-temperature Curie Weiss tail, with the temperature-independent paramagnetic response marked χ_0 . The blue line is a fit to Eq. 4.

suggest that NTSO remains within the fast fluctuation regime at all measured temperatures). At much lower temperatures, we speculate that the dilute distribution of electronic moments originates from unpaired spins due to defects and/or impurities.

To gain a rough estimate of n , the concentration of unpaired spins within the samples, from the μSR data, we followed the method used in Ref. 30. We assume the unpaired spins to have $S = 1/2$, given the spin of the Ti^{3+} ions, although a defect in a chain would produce two free spins and any impurity creating the defect may itself have a spin, so our value will be larger than the concentration of defects and impurities. Measurements were made in small magnetic fields, $\leq 5\text{mT}$ for NTSO and 2 mT and 10 mT for TiOCl, applied along the direction of the initial muon spin polarization, at low temperature. The asymmetry spectra were fitted using the product of a longitudinal field Kubo-Toyabe function²⁶ and an exponential relaxation to model the weak dynamics³⁰. Fitting the data to this function we can extract the width of the distribution of local fields at the muon site. From this we estimate the concentration of unpaired spins surrounding the muon using the expression given in Ref. 37 and adapted to the muon case in Ref. 30. For NTSO this gives an impurity concentration $n = 1.7(3)\%$, and for TiOCl we find $n = 1.1(2)\%$.

Magnetic susceptibility, χ , measurements (Fig. 2(b) and Fig. 3(b)) showed that our samples were comparable with those used in previous studies. From the low temperature Curie tail in χ we estimate the concentration of unpaired spins to be $n = 2.10(4)\%$ for NTSO and $0.6(1)\%$ for TiOCl. The close agreement between these values and those obtained from μSR sup-

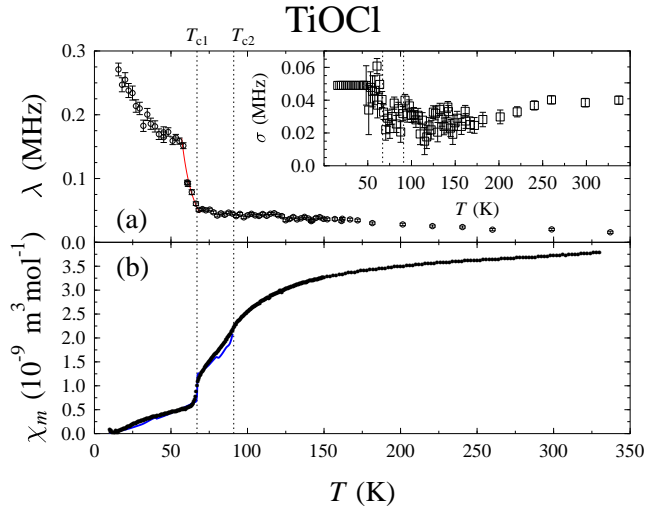


FIG. 3: (Color online) Fitted data for TiOCl . (a) Electronic relaxation rate, λ (Eq. 1). The red solid line is a fit to Eq. 2 between 58K and 68.2K, where the relaxation rate was found to be thermally activated. (Inset) Nuclear relaxation rate, σ , (Eq. 1) showing a weak temperature dependence³³. (b) Magnetic susceptibility, χ_m , after subtraction of the low-temperature Curie-Weiss tail. The solid blue line is the fit, described in the text, using the values of the dimerization parameter from Ref. 23 to define the temperature variation of the spin gap and applying Eq. 4 to describe the susceptibility.

ports our model describing the muon depolarization. The temperature-independent contribution to the susceptibility was $\chi_0 = 1.21(1) \times 10^{-9} \text{ m}^3 \text{ mol}^{-1}$ for NTSO, consistent with previous data⁵. For TiOCl we found that χ_0 was negligible, once the contribution to the susceptibility from the dimerization was considered. To extract the size of the spin gap from the magnetic susceptibility data, the Curie and temperature-independent terms were subtracted and we take the contribution, χ_m , due to the thermal activation of spins across the spin gap of magnitude 2Δ to be:

$$\chi_m = C \exp(-2\Delta/k_B T). \quad (4)$$

The result of fitting Eq. 4 to the data for NTSO is shown in Fig. 2(b). Using a constant value for the spin gap in NTSO, this gives an excellent parameterization of the data from low temperature to 200 K and leads to a value of the spin gap of $2\Delta = 595(7)$ K, somewhat smaller than the μSR measurements suggest. The situation in TiOCl is more complicated, since the dimerization varies strongly with temperature. The structural dimerization gives alternating exchange constants along the chain $J_{1,2} = J(1 \pm \delta)$ and we take δ to vary linearly with the structural dimerization³⁸. To model the form of the susceptibility we used the intensity of the superstructure reflection observed in X-ray diffraction measurements²³. For small values of δ the intensity of this peak varies as δ^2 . The spin gap is proportional³⁸ to $\delta^{2/3}$ and, using these results to convert the peak intensities into an ef-

TABLE I: Parameters derived from μ SR and magnetic susceptibility data, χ . The spin gap, 2Δ , the concentration of unpaired spins, n , and $T_{\text{mf}} = 2\Delta/3.53$, the temperature at which mean-field theory estimates that the SP transition should occur, given the value of 2Δ measured by μ SR.

Sample	NTSO	TiOCl
2Δ (K) μ SR	660(60)	420(40)
2Δ (K) χ	595(7)	-
n (%) μ SR	1.7(3)	1.1(2)
n (%) χ	2.10(4)	0.6(1)
T_{mf} (K)	190(20)	120(10)

fective spin gap, we then used Eq. 4 to derive the line plotted in Fig. 3(b). This was scaled by the spin gap value derived from the μ SR measurements and the constant C was chosen to fit the data, given we have no *a priori* values to choose for either case. A Curie-Weiss term was added to give the best fit to the low temperature data, a process complicated by oxygen adsorption, and so there remains a small discrepancy between the model and the data. Given that this model should only work in the limit $\Delta \gg T$,³⁸ it can be seen to be remarkably successful in describing the form of the data below 80 K, showing that the susceptibility is indeed varying with the structural dimerization. The breakdown of this model may explain why magnetic measurements suggest a lower value of T_{c2} than the XRD measurements.

In conclusion, we have measured the magnitude of the

spin gap using μ SR in the two Ti^{3+} chain compounds $\text{NaTiSi}_2\text{O}_6$ and TiOCl . Both the magnetic susceptibility and μ SR data for $\text{NaTiSi}_2\text{O}_6$ are well described by assuming that the spin gap is independent of temperature below the transition at $T_{\text{OO}} = 210$ K, and we find the magnitude of the spin gap, $2\Delta = 660 \pm 60$ K, to be consistent with magnetic susceptibility measurements (Table I) and recent theoretical work^{5,10,11}. TiOCl shows a thermally activated increase in the muon relaxation rate below $T_{c1} = 67$ K. Our value of $2\Delta = 420 \pm 40$ K is consistent with previous NMR data^{15,35} and optical measurements^{18,25}. Using mean-field theory to compare the measured spin gap in TiOCl to the observed transitions, we note (Table I) that $T_{\text{mf}} \simeq T^*$, the temperature where pseudogap formation has been observed^{15,18,25}, suggesting that T^* is analogous to T_{sp} in TiOCl , yet the system dimerizes at a far lower temperature. It is likely that the frustration between chains in the bilayer structure lowers the temperature at which dimerization occurs. In TiOCl we can directly relate previously reported superstructure reflections²³ to the magnetic susceptibility. Comparing the concentrations of unpaired spins determined by μ SR and magnetic susceptibility measurements (Table I) we find that for both compounds the two methods are consistent, although our assumptions suggest that both techniques overestimate the impurity concentration.

We are grateful to P. J. C. King and the staff of the ISIS Pulsed Muon facility for experimental assistance.

-
- ¹ J.W. Bray *et al.*, Phys. Rev. Lett. **35**, 744 (1975).
² M. Hase *et al.*, Phys. Rev. Lett. **70**, 3651 (1993).
³ S. Huizinga *et al.*, Phys. Rev. B **19**, 4723 (1979).
⁴ F.D.M. Haldane, Phys. Lett. **93A**, 464 (1983).
⁵ M. Isobe *et al.*, J. Phys. Soc. Jpn. **71**, 1423 (2002).
⁶ M. Shaz *et al.*, Phys. Rev. B **71**, 100405(R) (2005).
⁷ A. Seidel *et al.*, Phys. Rev. B **67**, 020405(R) (2003).
⁸ G.J. Redhammer *et al.*, Acta Cryst. **B59**, 730 (2003).
⁹ M.J. Konstantinović *et al.*, Phys. Rev. B **69**, 020409(R) (2004).
¹⁰ T. Hikihara and Y. Motome, Phys. Rev. B **70**, 214404 (2004).
¹¹ S.V. Streltsov *et al.*, Phys. Rev. Lett. **96**, 249701 (2006).
¹² J. van Wezel and J. van den Brink, Europhys. Lett. **75**, 957 (2006).
¹³ Z.S. Popović *et al.*, Phys. Rev. Lett. **93**, 036401 (2004).
¹⁴ Z.S. Popović *et al.*, Phys. Rev. Lett. **96**, 249702 (2006).
¹⁵ T. Imai and F.C. Chou, cond-mat/0301425 (unpublished).
¹⁶ J. Hemberger *et al.*, Phys. Rev. B **72**, 012420 (2005).
¹⁷ R. Rückamp *et al.*, Phys. Rev. Lett. **95**, 097203 (2005).
¹⁸ P. Lemmens *et al.*, Phys. Rev. B **70**, 134429 (2004).
¹⁹ V. Kataev *et al.*, Phys. Rev. B **68**, 140405(R) (2003).
²⁰ T. Saha-Dasgupta *et al.*, Europhys. Lett. **67**, 63 (2004).
²¹ M. Hoinkis *et al.*, Phys. Rev. B **72**, 125127 (2005).
²² D.V. Zakharov *et al.*, Phys. Rev. B **73**, 094452 (2006).
²³ A. Krimmel *et al.*, Phys. Rev. B **73**, 172413 (2006).
²⁴ A. Schönlieber *et al.*, Phys. Rev. B **73**, 214410 (2006).
²⁵ G. Caimi *et al.*, Phys. Rev. B **69**, 125108 (2004).
²⁶ S.J. Blundell, Contemp. Phys. **40**, 175 (1999).
²⁷ J.L. García-Muñoz *et al.*, Phys. Rev. B **52**, 4288 (1995).
²⁸ K.M. Kojima *et al.*, Phys. Rev. Lett. **79**, 503 (1997).
²⁹ S.J. Blundell *et al.*, J. Phys.: Condens. Matter **9**, L119 (1997).
³⁰ B.W. Lovett *et al.*, Phys. Rev. B **61**, 12241 (2000).
³¹ K. Kojima *et al.*, Phys. Rev. Lett. **74**, 3471 (1995).
³² H. Schaefer *et al.*, Z. Anorg. Allg. Chem. **295**, 268 (1958).
³³ While there was no trend in the temperature dependence, there were significant fluctuations in the value of σ measured in TiOCl , and so it was left as a free parameter whilst fitting the data. We include data from two separate experiments and the slight change in the relaxing background strongly affected σ , despite the fact that the values of λ were in excellent agreement.
³⁴ E. Ehrenfreund and L.S. Smith, Phys. Rev. B **16**, 1870 (1977).
³⁵ The model of Ref. 34, describing NMR data, implies that the Δ value measured in Ref. 15 corresponds to 2Δ in the conventional notation.
³⁶ Y.J. Uemura *et al.*, Phys. Rev. B **31**, 546 (1985).
³⁷ R.E. Walstedt and L.R. Walker, Phys. Rev. B **9**, 4857 (1974).
³⁸ M.C. Cross and D.S. Fisher, Phys. Rev. B **19**, 402 (1979).

